Article citation info:
LATALSKI J: Modelling of macro fiber composite piezoelectric active elements in ABAQUS system. Eksploatacja i Niezawodnosc - Maintenance and Reliability 2011; 4: 72-78.

Jarosław LATALSKI

MODELLING OF MACRO FIBER COMPOSITE PIEZOELECTRIC ACTIVE ELEMENTS IN ABAQUS SYSTEM

MODELOWANIE W SYSTEMIE ABAQUS PIEZOELEKTRYCZNYCH ELEMENTÓW AKTYWNYCH TYPU MFC*

The paper presents an approach to effective modelling of piezoelectric transducers in finite element method based software. A macroscopic model of an active element made of macro fiber composite (MFC type) exhibiting d_{33} effect is developed in ABAQUS system. Next, a multilayer composite beam with the discussed piezoelectric actuator is analysed. Both a direct and a converse piezo effects are analyzed numerically, calculating respectively charge on transducer's poles subject to forced displacements and beam static deflections with respect to assumed supply voltage. The outcomes of the numerical simulations are compared to the laboratory test results. Next, the worked-out FEM model of MFC actuator/sensor is used to detect the simulated defect in composite material.

***Keywords**: piezoelectric transducer, active elements, FEM, ABAQUS.*

W pracy przedstawiono sposób efektywnego modelowania kompozytowych elementów piezoelektrycznych metodą elementów skończonych. W systemie ABAQUS przygotowano makroskopowy model elementu aktywnego typu MFC wykorzystującego efekt piezoelektryczny d_{33}. W dalszej kolejności przeanalizowano wielowarstwową belkę kompozytową z naklejonym badanym elementem aktywnym. Numerycznie zbadano prosty i odwrotny efekt piezoelektryczny, wyznaczając odpowiednio wartości napięć na zaciskach elementu aktywnego przy wymuszonym odkształceniu układu oraz ugięcia statyczne przy różnych wartościach napięcia zasilającego. Rezultaty tych analiz porównano z wynikami rzeczywistych pomiarów przeprowadzonych na stanowisku laboratoryjnym. Opracowany model numeryczny wykorzystano do próby wykrycia symulowanego uszkodzenia materiału kompozytowego.

***Słowa kuczowe**: przetwornik piezoelektryczny, elementy aktywne, metoda elementów skończonych, ABAQUS.*

1. Introduction

Since 80s one observes a significant increase of interest in a class of systems that started to be called 'intelligent'. This group contains shape memory alloys (SMA), magneto- and electrorheological fluids (MRF, ERF) and piezoelectrics. Common examples of the last ones are lead zirconate titanate – PZT, barium titanate – $BaTiO_3$ and polyvinylidene fluoride polymer – PVDF. As the piezoelectrics gradually started to become widespread, in mid-90s the research activities were aimed at using PZTs for structural health monitoring and structural reliability assessment. One of the most promising directions is related to an application of piezoceramics [3], [4] and micro fiber composites. The results of already carried out projects confirm a high suitability of MFC type elements not only for structural health monitoring but for vibration suppression, energy harvesting etc. as well [9], [11].

It should be emphasized, that most of the current research projects are focused not only on structural testing in laboratories or in real operating conditions. An attention is given to the analysis and design of structural health monitoring systems by means of numerical simulations [5].

The crucial problem in analysis and design of structures with piezoelectric elements are interactions between mechanical and electrical phenomena – see relations (1) and (2). Therefore, the exact analytical solution of constitutive equations is possible only for the simplest models e.g. symmetric discs under static load or at resonance conditions. The analytical solutions for more complex geometries and loadings require radical simplifications. This leads to serious discrepancies between predicted and observed systems' responses [7].

The complexity of the discussed phenomena involves the usage of approximate approaches to the design. Numerical methods, and especially a finite element method seems to be a natural choice. The main advantage of this approach is a possibility of modelling complex phenomena by the division of a domain into simple elements, where the solution of equilibrium equations is possible. Although the first libraries of piezo-elements were implemented into finite element software in late eighties, these are still available only in selected FEM systems.

Following the above observations the aim of this paper is to develop an effective macroscopic finite element modelling of piezoelements made of macro fiber composites. It is expected,

(*) Tekst artykułu w polskiej wersji językowej dostępny w elektronicznym wydaniu kwartalnika na stronie ***www.ein.org.pl***

that the proposed method will enable further simulation research on using MFC transducers for structural health monitoring task – e.g. detecting delamination (as series of experiments presented in [8]), crack propagation etc. Moreover, numerical simulations of changing machines' operating conditions, like vibration restraining, might be possible.

2. Mathematical models of piezoelectric materials

Implementation of piezoelectric transducers in engineering structures requires not only detailed information about their strength data but characteristics of their behaviour under mechanical and electrical loads as well.

One of the first researches aiming at developing linear constitutive equations of piezoelectric materials (LPCE) are models elaborated by D.A. Berlincourt and D.R. Curran and later by H. Jaffe [12]. Several phenomena like coercion effect and changes in crystallographic structure are left out of account during the derivation, but because of linearity of piezoelectricity phenomena within the range of small and medium electrical fields, these models describe the behaviour of real systems quite accurately and are still in common usage today.

The constitutive equations describing the piezoelectric property are based on the assumption that the total strain in the transducer is the sum of mechanical strain induced by the mechanical stress and the strain caused by the applied electric voltage. The model is formulated as a pair of two matrix relations (according to Mandel-Voigt notation), describing the interactions of mechanical and electrical phenomena [6]:

$$\boldsymbol{\varepsilon} = \mathbf{S}^E\boldsymbol{\sigma} + \mathbf{d}^{\mathrm{T}}\mathbf{E} \tag{1}$$

$$\mathbf{D} = \mathbf{d}\boldsymbol{\sigma} + \boldsymbol{\xi}^{\sigma}\mathbf{E} \tag{2}$$

where: $\boldsymbol{\varepsilon}$ — strain vector (−), $\mathbf{S}^E$ — compliance matrix (m²/N) at constant electric field, σ — stress vector (N/m²), **d** — matrix of piezoelectric strain constants (m/V), **E**— electric field matrix (V/m), **D** — vector of electric displacements (C/m²), ξ^{σ}— matrix of permittivity coefficients (F/m = C/m·V) at constant stress.

The first of the above relations represents the converse piezoelectric effect i.e. the strain of the sample under the electric field load. This corresponds to the device being used as an actuator. The second equation (2) deals with the opposite case, when the transducer is being used as a sensor (direct piezoelectric effect). The given above notation is named to be a displacement-based formulation — the dependent variable is strain vector (tensor).

The system of equations (1)–(2) might be written also in another form — the so called force-based formulation:

$$\boldsymbol{\sigma} = \mathbf{C}^E\boldsymbol{\varepsilon} - \mathbf{e}^{\mathrm{T}}\mathbf{E} \tag{3}$$

$$\mathbf{D} = \mathbf{e}\boldsymbol{\varepsilon} + \boldsymbol{\xi}^{\varepsilon}\mathbf{E} \tag{4}$$

where: $\mathbf{C}^E$ – elastic stiffness matrix (N/m²) calculated at constant electric field, **e** – piezoelectric stress coefficients matrix (N/m·V = C/m²) (T denotes matrix transposition), and $\boldsymbol{\xi}^{\varepsilon}$ – matrix of dielectric permittivity coefficients (F/m) calculated at constant strain.

The force based formulation is frequently used for e.g. problems solved by finite element method, where the displacements (strain ε) are a primary variable and all the remaining quantities are ε dependent. In other problems — e.g. in case of analysis of thin plates in plane stress state the displacement based formulation might be more reasonable.

Therefore there are two matrices of piezoelectric coeffcients d_{ij} i e_{ij} defined as follows:

$$\begin{aligned} d_{ij} &= \left(\frac{\partial D_i}{\partial \sigma_j}\right)^E = \left(\frac{\partial \varepsilon_j}{\partial E_i}\right)^{\sigma} \\ e_{ij} &= \left(\frac{\partial D_i}{\partial \varepsilon_j}\right)^E = -\left(\frac{\partial \sigma_j}{\partial E_i}\right)^{\varepsilon} \end{aligned} \tag{5}$$

which are related to each other by material constants matrix:

$$\mathbf{d} = \mathbf{e}\mathbf{S}^E \tag{6}$$

It should be underlined that the piezoelectric coefficients matrices **d** and **e** are determined not only at constant electric field and strain or stress respectively (*E,* ε and σ), but also at a constant temperature. Although detailed tests show that piezoelectric coefficients are temperature dependent, in practical applications it is assumed that this influence on piezoelectric coefficients, as well as on other material data, is negligible.

For 3-D systems equations (1-2) after expansion are:

$$\begin{bmatrix} \varepsilon_1 \\ \varepsilon_2 \\ \varepsilon_3 \\ \varepsilon_4 \\ \varepsilon_5 \\ \varepsilon_6 \\ D_1 \\ D_2 \\ D_3 \end{bmatrix} = \begin{bmatrix} S_{11} & S_{12} & S_{13} & S_{14} & S_{15} & S_{16} & d_{11} & d_{21} & d_{31} \\ S_{21} & S_{22} & S_{23} & S_{24} & S_{25} & S_{26} & d_{12} & d_{22} & d_{32} \\ S_{31} & S_{32} & S_{33} & S_{44} & S_{35} & S_{36} & d_{13} & d_{23} & d_{33} \\ S_{41} & S_{42} & S_{43} & S_{44} & S_{45} & S_{46} & d_{14} & d_{24} & d_{34} \\ S_{51} & S_{52} & S_{53} & S_{54} & S_{55} & S_{56} & d_{15} & d_{25} & d_{35} \\ S_{61} & S_{62} & S_{63} & S_{64} & S_{65} & S_{66} & d_{16} & d_{26} & d_{36} \\ d_{11} & d_{12} & d_{13} & d_{14} & d_{15} & d_{16} & \xi_{11} & \xi_{12} & \xi_{13} \\ d_{21} & d_{22} & d_{23} & d_{24} & d_{25} & d_{26} & \xi_{21} & \xi_{22} & \xi_{23} \\ d_{31} & d_{32} & d_{33} & d_{34} & d_{35} & d_{36} & \xi_{31} & \xi_{32} & \xi_{33} \end{bmatrix} \cdot \begin{bmatrix} \sigma_1 \\ \sigma_2 \\ \sigma_3 \\ \sigma_4 \\ \sigma_5 \\ \sigma_6 \\ E_1 \\ E_2 \\ E_3 \end{bmatrix} \tag{7}$$

The terms (S_{11},S_{22},...ξ_{33}) located at the main diagonal represent strictly mechanical and electrical effects. The reciprocal coupling of these two domains is given by d_{ij} parameters located outside of the main diagonal. These values correspond to the effect of deformation caused by electric field and charge induction resulting from material's stress. Therefore these coefficients are often used to compare the 'power' of different piezoelectric materials between each other.

The given above system of equations is significantly simplified for materials exhibiting 4mm crystalline class (e.g. lead zirconate titanate – PZT, barium titanate – $BaTiO_3$) or 6mm one [6]. This is related to the symmetry of elastic, electric and electro-mechanic properties. Assuming – according to ANSI IEEE 176 standards – that the device is poled along the 3 axis and that the piezoelectric material is a transversely isotropic one (1-2 beeing the plane of transverse isotropy) the constitutive equations (7) might be simplified to:

$$\begin{bmatrix} \varepsilon_1 \\ \varepsilon_2 \\ \varepsilon_3 \\ \varepsilon_4 \\ \varepsilon_5 \\ \varepsilon_6 \\ D_1 \\ D_2 \\ D_3 \end{bmatrix} = \begin{bmatrix} S_{11} & S_{12} & S_{13} & 0 & 0 & 0 & 0 & 0 & d_{31} \\ S_{21} & S_{11} & S_{13} & 0 & 0 & 0 & 0 & 0 & d_{31} \\ S_{31} & S_{31} & S_{33} & 0 & 0 & 0 & 0 & 0 & d_{33} \\ 0 & 0 & 0 & S_{55} & 0 & 0 & 0 & d_{15} & 0 \\ 0 & 0 & 0 & 0 & S_{55} & 0 & d_{15} & 0 & 0 \\ 0 & 0 & 0 & 0 & 0 & 2(S_{11}-S_{12}) & 0 & 0 & 0 \\ 0 & 0 & 0 & 0 & d_{15} & 0 & \xi_{11} & 0 & 0 \\ 0 & 0 & 0 & d_{15} & 0 & 0 & 0 & \xi_{22} & 0 \\ d_{13} & d_{13} & d_{33} & 0 & 0 & 0 & 0 & 0 & \xi_{33} \end{bmatrix} \cdot \begin{bmatrix} \sigma_1 \\ \sigma_2 \\ \sigma_3 \\ \sigma_4 \\ \sigma_5 \\ \sigma_6 \\ E_1 \\ E_2 \\ E_3 \end{bmatrix} \tag{8}$$

Most of the commercially available active elements exhibit a d_{33} effect or d_{31} one. The d_{33} effect corresponds to the deformation of a specimen in the direction of driving electric field (also

poling direction); whereas in the second case the deformation occurs in the plane perpendicular to the electric field vector.

3. Numerical model of the piezoelectric element and its verification

For numerical and laboratory tests M-8503-P1 element made by Smart Material Corp., Sarasota (FL) USA is used – see figure 1. This is the transducer of d_{33} effect type.

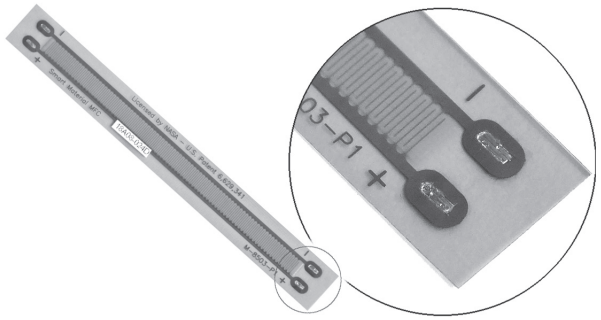

Fig. 1. Active element M-8503-P1 made by Smart Material Corp., Sarasota (FL) USA

Despite of modular structure of the transducer under consideration (170 sections of electrocouples distant by 0.5 mm from each other – see zooming area in figure 1) the piezoelement hasn't been modelled in micro scale. The aim of the paper is to develop a simplified but effective method of modelling, assuring results consistent with manufacturer's data and laboratory experiments.

Therefore, in the presented approach a supplementary body made of orthotropic, homogenous piezoelectric material is proposed, where voltage is applied to opposite specimen faces. The transducer's domain is modelled in ABAQUS software by the solid continuum elements C3D20E, i.e. 20-nodal second order, having four degrees of freedom in each node. Three DOF are translational and the fourth one is an electric charge directly related to the piezoelectric properties of the material.

According to the data provided by the manufacturer the value of d_{33} coefficient in M-8503-P1 element is not constant with respect to the electric field. For $|E| < 1$ kV/mm the parameter d_{33} equals $400 \cdot 10^{-12}$ m/V, for higher magnitude fields ($|E| > 1$ kV/mm) the d_{33} increases to $460 \cdot 10^{-12}$ m/V (all these data are given for a single couple of electrodes). Following this information the provided d_{33} values have to be multiplied by the number of sections in M-8503-P1 element (Figure 1) to get the effective value to be put into the FEM model for preliminary calculations. This has been done to set trial values of piezoelectric coefficients.

The remaining elastic and ferroelectric properties are taken from the manufacturer catalog:

- elastic orthotropic material given by Young's moduli $E_1 = E_2 = 15857$ MPa, $E_3 = 30336$ MPa, Kirchhoff's moduli $G_{12} = G_{13} = G_{23} = 5515$ MPa and Poisson's ratios $\nu_{12} = \nu_{13} = \nu_{23} = 0{,}31$,
- isotropic ferroelectric material with constant permittivity $\xi = 8 \cdot 10^{-9}$ F/m coefficients on the main diagonal. All the out-of-diagonal terms in ξ matrix are neglected (see equation (8)).

Numerical model validation

Verification of the piezoelectric element model is done by means of two tests given in manufacturer's documentation. In the first numerical experiment strains for a free element under specified driving voltage are calculated and compared to catalog data. In the second experiment – called blocking force test – the force exerted by the piezoelement with excluded deformations is calculated and compared to the reference value.

Mechanical and electrical boundary conditions for the conducted tests are set as follows:

- free strain test – nodes located at the bottom face of the piezoelectric specimen are allowed to move only in *xy* plane, nodes located at one of the lateral longitudinal faces are restricted to move in *yz* plane only. Finally, one of lateral transversal faces gets the support along *y* direction and, additionally, constant electric potential 0 V is kept there. Charge potential of 1500 V is applied along the specimen length. These conditions are presented in figure 2.
- blocking force test – same boundary conditions as in the previous experiment with additional constraint $u_y = 0$ for the nodes on the opposite, transverse (short) face.

Results of initial numerical tests shows a serious discrepancy comparing to the catalogue data. In free strain test the error is 16-31% – axial strains $1206\text{-}1363 \cdot 10^{-6}$ with respect to reference value $\varepsilon_y = 1050 \cdot 10^{-6}$; in blocking force test the error is 17-33% – i.e. +32,7-+37,58 N with respect to 28.00 N. Therefore, in order to achieve a satisfactory accuracy the correction of the effective piezoelectric coefficient is necessary. Minimising the relative error in both tests as a function of d_{33} parameter its optimal value for the M-8503-P1 element is found to be $59 \cdot 10^{-9}$ m/V. After this correction strains calculated in the first test are $1040 \cdot 10^{-6}$ (vs $1050 \cdot 10^{-6}$ by manufacturer); force for blocked element is $R_y = 28.46$ with respect to 28.00 N in documentation. Therefore,

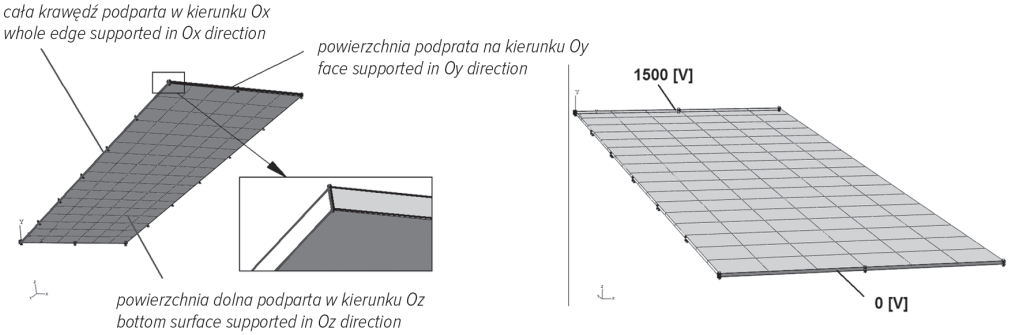

Fig. 2. Boundary conditions in computations validating the model of an examined transducer

the results of the final simulations for the updated d_{33} parameter prove the piezoelectric patch model and modelling technique for MFC transducers to be correct.

4. Analysis of a composite beam with piezoelectric patch

To present the potential of the proposed effective piezoelement modelling technique two experiments are performed. In the first one a reference composite beam with bonded patch of M-8503-P1 active element is analysed. Experiments representing both direct and converse piezoelectric effects are run. Within the frame of these voltage at transducer's poles is recorded for forced beam bending and next displacements of a specified point on specimen resulting from voltage applied to PZT patch. Results of laboratory experiments are compared to the outcomes of numerical calculations in ABAQUS system. In performed simulations the previously derived and verified finite element model of the transducer is used.

Second stage of research comprises the analysis of the composite beam with a simulated material defect. Damage corresponding to broken composite fibers (or their pull-out from matrix resulting from adhesive joint failure) is simulated as a local change in composite material stiffness. Specimen with this simulated defect is tested numerically. Within the tests programme voltage induced on transducer poles with respect to forced specimen bending is recorded. Outcomes are related to the data for an undamaged (healthy) sample.

4.1. Model and sample specimen testing

The verified model of the piezoelectric transducer is used to simulate the static response of composite cantilever beam with M-8503-P1 active element. The basic beam is made of unidirectional glass fibers tape and epoxy Prime 20 (Sicomin 8100 + hardener 8824, fibers ratio 50±2% – according to manufacturer Macro Composites, UK data). The subsequent layers of the composite are set in the following order: 0°/90°/+45°/-45°/+45°/90°/0° (with respect to O*y* axis pointing along the beam length). Piezoelement M-8503-P1 is bonded on the upper face of a specimen, directly at the clamped end. Draft view of a structure under consideration is given in figure 3 (all dimensions in mm).

Composite model of the beam is defined as a lamina type one. This approach enables modelling of a composite as a set of orthotropic layers in plane-stress state. In numerical simulations the following data provided by the manufacturer of a composite is used: Young modulus along fibers E_1 = 20 000 MPa, transversal Young modulus E_2 = 2 000 MPa, shear moduli $G_{12} = G_{13} = G_{23}$ = 9 800.7 MPa and Poisson's ratio ν_{12} = 0.26. The ABAQUS finite element model based on shell elements is made according to Layup-Ply technique [1]. In the analysis S8R elements are used – i.e. second order ones with reduced integration.

The piezoceramic material properties are defined as described in previous section of the paper; the already verified piezoelectric coefficient $d_{33} = 59.0 \cdot 10^{-9}$ m/V is used in further simulations. All the remaining (i.e. out-of-diagonal) coefficients of **d** matrix are set to be 0. According to manufacturer data and actual measurements the active area of an element is set to 85×3 mm. Next, the model of a piezoelement is 'glued' to master structure by TIE constraints method, which results in joining appropriate DOF of both bodies. The mechanical boundary conditions are set by encastring the nodes on shorter side face of a beam. The final FEM model consists of 317 elements (beam 300, piezoelectric element 17) and 1243 nodes; this results in 7034 degrees of freedom. The finite element model of the structure and composite stacking sequence is presented in figure 4.

During the static analysis of the piezo-composite system a series of simulations is run. Subsequent loadings within the range of 0-1500 V are applied to the positive terminal of the

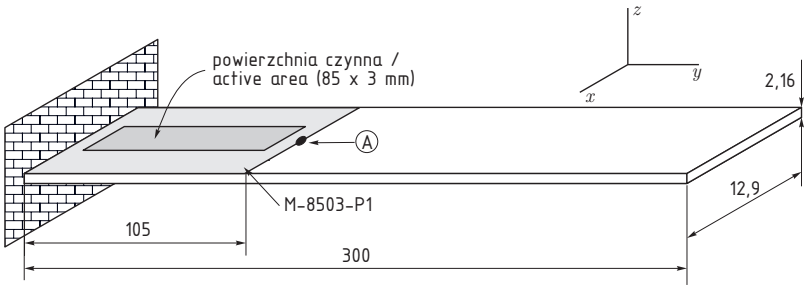

Fig. 3. Scheme of the composite beam under consideration

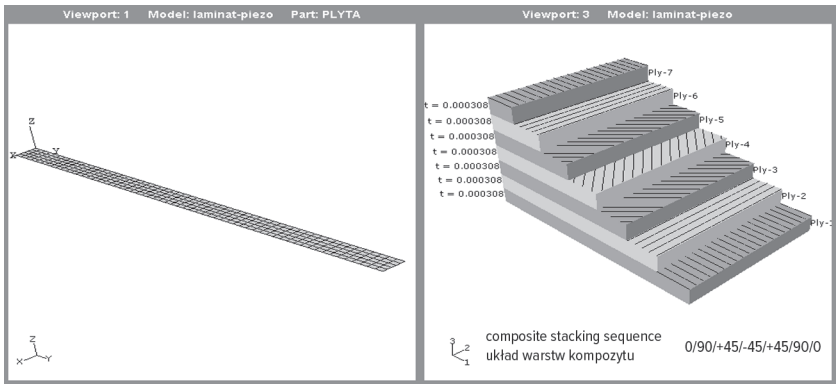

Fig. 4. Discrete model of the composite beam and layout of individual layers (orientation of fibers in direction 1 corresponds to Oy axis

transducer, keeping the constant value of 0 V at a negative one (see figure 2). The deflections of a beam are calculated by reporting the vertical displacement of a point located at the edge of the piezoelement (see point A in figure 3). A converse piezoelectric effect is also tested – i.e. calculating electrical potential on transducer terminals with respect to forced beam bending.

4.2. Laboratory tests

To verify the presented above approach to modelling systems of composite structures with piezoelements an experimental stand has been prepared in the Laboratory for Dynamics and Strength of Materials at the Lublin University of Technology. The setup, shown in figure 5, consists of a uniform composite cantilever beam with a single piezoelectric transducer laminated onto the upper face. The transducer is connected to D.C. power unit with a controllable resistance divider. The requested voltages are provided by a high-voltage amplifier model PA05039 made by Smart Materials company. At the second stage of tests a converse problem is examined. During these a micrometer screw is used to deflect the composite beam, meanwhile voltages induced by the piezoelement are recorded.

4.3. Results statement

Results of numerical calculations are presented in the following figures. Figure 6 presents a shape of the beam in bending calculated by ABAQUS for three different driving voltages: 500 V, 1000 V and 1500 V. Horizontal axis is aimed along beam length (O*y* – left end clamped) and vertical axis corresponds to beam transversal displacements; all data are given in mm.

Figure 7 presents the statement of numerical and laboratory tests for the converse piezoelectric effect. The vertical translations of a point located at the external edge of the transducer (see point A in figure 3) are compared. The deflections are collected for several driving voltages.

Figure 8 presents the results of direct piezoelectric effect testing. The assumed a'priori beam deflection has been forced by micrometer screw, meanwhile the voltage at transducer's poles is recorded. These experimental results are compared to simu-

Fig. 5. General view of the test stand

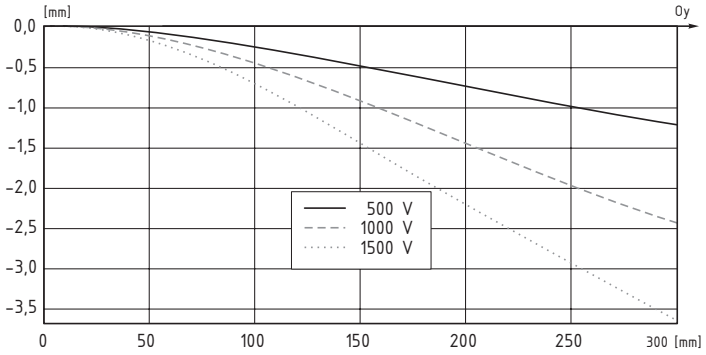

Fig. 6. Deflection of the tested specimen at different driving voltages (numerical sumulation)

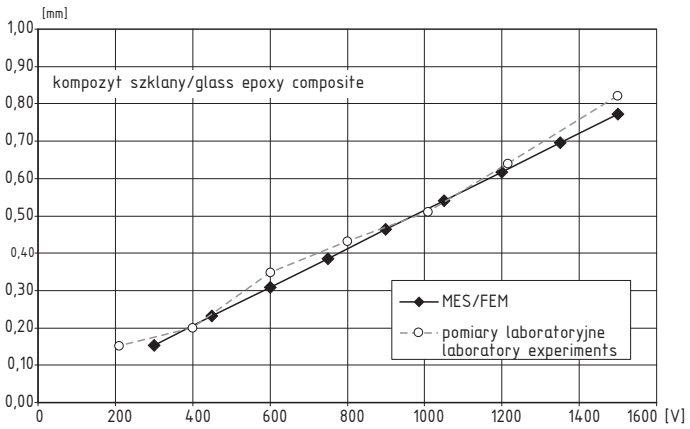

Fig. 7. Vertical translations of point A obtained from numerical simulations and laboratory tests of composite beam with piezoelement for different driving voltages

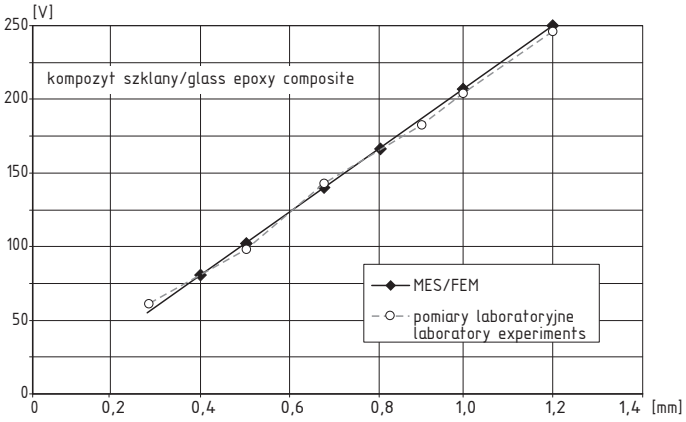

Fig. 8. Comparison of numerical simulations and laboratory tests of a converse piezoelectic effect for the specimen under consideration

lations in ABAQUS system run on models prepared according to proposed technique.

In all discussed cases a high accuracy of simulations and laboratory test is achieved. For the examined points the calculated differences do not exeed 6%.

4.4. Numerical test of a damaged composite beam

Results of the above tests induced an idea of using the proposed macroscopic modelling technique of MFC type tranducers for detecting composite material damage. The simulated material defect corresponds to composite fibers breaking (or their pull-out from matrix resulting from adhesive joint failure).

Macroscopic, simplified representation of this type of material damage consists in partial fiber 'removal' from constitutive equations, and next from the formula for effective longitudinal and shear stiffness laminae moduli [2]. Assumung the fibers to be oriented along O*x* axis, the effective lamina stifnesses moduli are calculated according to the rule of mixtures as follows [10]:

$$\begin{aligned} E_{xx} &= E_f V_f + E_m V_m \\ E_{yy} &= E_m \frac{1+\alpha V_f}{1-V_f} \\ \nu_{xy} &= V_f \nu_f + V_m \nu_m \end{aligned} \tag{9}$$

where subscripts x and y denote principal directions, V denotes volumetric ratio of a constitutent, index „f" denotes fiber, index „m" matrix. Coefficient α is given by:

$$\alpha = \frac{E_f / E_m - 1}{E_f / E_m + 1} \tag{10}$$

Following the above equations it's possible to formulate the constitutive equations for the damaged composite material, where the altered longitudinal stiffenesses (9) need to be used.

Denoting the volume of broken fibers in the damaged material by V_{df}, value of stiffness moduli E are decreased according to the following formula [2]:

$$E_{xx} = E_f V_{df} + E_m (1 - V_{df}) \qquad E_{yy} = E_m \frac{1+\alpha V_{df}}{1-V_{df}} \tag{11}$$

For finite element calculations the previously tested and verified numerical model of the composite beam with the PZT patch is used. Composite material damage is simulated by decreasing the lamina stiffness on the 20 mm long section, starting at 2 mm distance from the clamped edge. It has been assumed that the volumetric ratio V_{df} of damaged fibers in composite material equals to 0.25. In performed numerical tests the electric potential at transducer's poles is calculated subject to forced vertical deflection of point A (see figure 3). The outcomes of the simulation are compared to the results of similar tests run on the undamaged system. The relevant results are presented graphically – see figure 9.

The obtained results indicate, that the calculated voltages, in the whole tested range, are approximately 8% lower while comparing to the reference (healthy) system. These differences exceed the error resulting from the comparison of a reference system and laboratory tests outcomes.

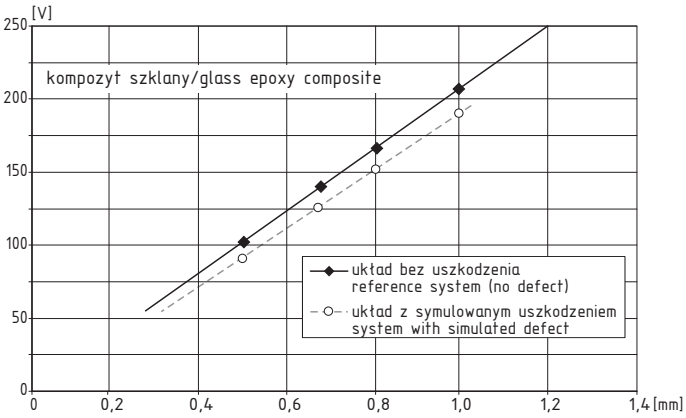

Fig. 9. Results of numerical test of a composite beam with simulated material defect

6. Conclusions

The paper presents the possibilities of effective modelling of MFC type piezoelectric transducers exhibiting d_{33} effect. A high correlation of numerical results and the outcomes of laboratory tests is achieved. In none of the examined cases the error exeeded 6%. This observation confirms the validity of derived macroscopic approach to finite element modelling of MFC type transducers and also validity of suggested discretisation of the specimen domain.

The outcomes of these initial investigations encourage for further numerical simulation research using the derived and already verified modelling technique. These might focus on finite element method structural health monitoring by means of dynamic methods – especially modal analysis and wave propagation. The next stage might be modelling of plates and shells. Multiple piezoelements used as sensors and actuators seems to be of particular interest too.

****

The financial support of the Structural Founds in the Operational Programme Innovative Economy (IE OP) financed from the European Regional Development Found – research project "Modern material technologies in aerospace industry" number POIG.0101.02-00015/08 is gratefully acknowledged.

****

7. References

1 Abaqus 6.9 Documentation.
2 Adams D E. Health Monitoring of Structural Materials and Components: Methods and Applications. Hoboken (NJ): John Wiley & Sons, 2007.
3 Kabeya K. Structural Health Monitoring Using Multiple Piezoelectric Sensors And Actuators. Blacksburg (VA): Virginia Polytechnic Institute and State University, 1998.
4 Kessler S S. Piezoelectric-Based In-Situ Damage Detection of Composite Materials for Structural Health Monitoring Systems. PhD thesis. Boston (MA): Massachusetts Institute of Technology, 2002.
5. Klepka T, Dębski H, Rydarowski H. Characteristics of high-density polyethylene and its properties simulation with use of finite element method. Polimery 2009; 54(9): 668-672.
6 Leo D J. Engineering Analysis of Smart Material Systems. Hoboken (NJ): John Wiley & Sons, 2007.
7 Lowrie F, Cain M, Stewart M. Finite Element Modelling of Electroceramics. Technical Report, A150. Teddington: Centre for Materials Measurement and Technology, National Physical Laboratory, 1999.
8 La Saponara V, Horsley D A, Lestari W. Structural Health Monitoring of Glass/Epoxy Composite Plates Using PZT and PMN-PT Transducers. ASME Journal of Engineering Materials and Technology 2011; 133(1): 011011.
9 Schönecker A J, Daue T, Brückner B, Freytag Ch, Hähne L, Rödig T. Overview on macrofiber composite applications. Proceedings of the SPIE – Smart Structures and Materials 2006 (ed. Armstrong WD) 2006; 6170: 408-415.
10 Kollar L, Springer G S. Mechanics of Composite Structures. Cambridge: Cambridge University Press, 2003.
11 Varadan V K, Vinoy K J, Gopalakrishnan S. Smart Material Systems and MEMS: Design and Development Methodologies. Chichester (NH): John Wiley & Sons, 2006.
12 Yousefi-Koma A. Intelligent Materials. W: Piezoelectric Ceramics as Intelligent Multifunctional Materials: 231-254. Cambridge: The Royal Society of Chemistry Publishing, 2008.

Jarosław LATALSKI, Ph.D. Eng.
Department of Applied Mechanics
Faculty of Mechanical Engineering
Lublin University of Technology
36 Nadbystrzycka Str., 20-618 Lublin, Poland
e-mail: j.latalski@pollub.pl